Available online at www.sciencedirect.com
ScienceDirect
Ceramics International 36 (2010) 1467–1472
CERAMICS INTERNATIONAL
www.elsevier.com/locate/ceramint

Short communication

Ti^{4+} addition effect on α-Al_2O_3 flakes synthesis using a mixture of boehmite and potassium sulfate

Hsing-I. Hsiang *, Chia-Che Chuang, Tsung-Hao Chen, Fu-Su Yen

Department of Resources Engineering, Particulate Materials Research Center, National Cheng Kung University, Tainan 701, Taiwan

Received 2 November 2009; received in revised form 11 November 2009; accepted 16 December 2009
Available online 28 January 2010

Abstract

Single-crystal α-Al_2O_3 hexagonal flakes with a diameter of about 200 nm and 20 nm in thickness were obtained by mixing different molar ratios of potassium sulfate to boehmite and heating at 1000 °C. Co-doping 1 mol% TiO_2 can increase the shape anisotropy of α-Al_2O_3 hexagonal flakes, increasing the diameter to 400 nm. The effects of potassium sulfate, Fe_2O_3 and TiO_2 on the phase transformation and morphology development of alumina were investigated using X-ray diffraction analysis (XRD), differential thermal analysis (DTA) and transmission electron microscopy (TEM). The results indicate that co-doping potassium sulfate, Fe^{3+} and Ti^{4+} can promote γ → α-Al_2O_3 phase transformation and change the morphology from a vermicular structure into hexagonal platelets. The shape anisotropy of α-Al_2O_3 hexagonal flakes can be increased by adding TiO_2 due to the segregation of Ti^{4+} ions onto the surfaces of basal planes of α-Al_2O_3 single crystal particle.

Keywords: Flake; α-Al_2O_3; Potassium sulfate; TiO_2

1. Introduction

α-Al_2O_3 platelet powder has been widely applied in the industry, such as in metal or ceramic composite reinforcements [1,2], fillers in plastics for thermal conductivity enhancement [3], and pearlescent pigments [4], etc. Many methods have been used to prepare α-Al_2O_3 platelet powder, including heating a mixture of Al_2O_3 and aluminum fluoride [5], growth in an HF-γ-Al_2O_3 system [6], synthesis in a molten Na_2SO_4 flux [7,8], K_2SO_4 flux [9], synthesis in a 1,4-butanedial solution by seeding [10], synthesis using electrostatic spray-assisted chemical vapor deposition [11], and synthesis using the flux method in a microwave field [12].

In our previous study, we observed that single-crystal α-Al_2O_3 hexagonal platelets can be prepared by heating a mixture of boehmite and potassium sulfate at below the salt melting temperature [13]. However, the shape anisotropy (diameter: 200 nm and thickness: 25 nm) is too low to significantly improve the mechanical and optical properties of composites.

In this study, the effects of the additives on the phase transformation and morphology development of alumina were investigated. The formation mechanism of α-Al_2O_3 hexagonal flakes was also examined.

2. Experimental

The feed stock materials were all technical grade $Fe(NO_3)_3{\cdot}9H_2O$, boehmite, $TiCl_4$ and K_2SO_4. 94 mol% boehmite, 5 mol% $Fe(NO_3)_3{\cdot}9H_2O$, and 1 mol% $TiCl_4$ aqueous solution were mixed and then dried at 120 °C. The dried gel powder was sieved through # 200 mesh, and was denoted as 1T. Sample 1T was mixed with different molar ratios of a potassium sulfate solution, followed by drying at 120 °C and calcined at 1000 °C (the heating rate was 4 °C/min, maintained for 2 h, and cooled in an oven furnace). The samples compositions and notations used in this study are shown in Table 1. After calcination, the samples were washed with distilled water thoroughly to remove the potassium sulfate. The washed powder was dried at 120 °C and then subjected to analysis. The thermal properties of the samples were measured by DTA (Netzsch STA 409C). The crystalline phase evolution was characterized by an X-ray diffraction analysis with a CuKα radiation (Siemens, D5000). The size and morphology of the

* Corresponding author. Tel.: +886 6 2757575x62821; fax: +886 6 2380421.
E-mail address: hsingi@mail.ncku.edu.tw (H.-I. Hsiang).

0272-8842/$36.00
doi:10.1016/j.ceramint.2010.01.004

Table 1
Sample compositions and notations used in this study.

Samples	No.
95%Boehmite + 5% Fe^{3+}	0T
94%Boehmite + 5% Fe^{3+} + 1% Ti^{4+}	1T
(95%Boehmite + 5% Fe^{3+})/XK_2SO_4	0T*X*K (X = 1–4)
(94%Boehmite + 5% Fe^{3+} + 1%Ti^{4+})/XK_2SO_4	1T*X*K (X = 1–4)

powders were determined using TEM (JEOL JEM-3010, Tokyo, Japan). Semi-quantitative determination of the element content was detected by EDS (Noran, Voyager 1000), attached to the TEM.

3. Results and discussion

3.1. Effects of additives on the thermal behavior and phase transformation of boehmite

Fig. 1 shows the DTA curves for boehmite added with various Fe^{3+}, Ti^{4+}, and K_2SO_4 molar ratios. The endothermic peak at 500 °C and the exothermic peak at 1230 °C for pure boehmite are due to dehydration and $\theta \rightarrow \alpha$-$Al_2O_3$ phase transformation, respectively (Fig. 1(b)). For boehmite added with 5 mol% Fe^{3+}, sample 0T, the phase transformation temperature of $\theta \rightarrow \alpha$-$Al_2O_3$ decreased to 1041 °C, falling by about 189 °C compared with pure boehmite. It was reported [14] that at 500–600 °C, Fe^{3+} ions added in the boehmite were crystallized into hematite, which can act as a seed to decrease the activation energy of the $\theta \rightarrow \alpha$-$Al_2O_3$ phase transformation, hence decreasing the phase transformation temperature. The Fe effects on formation of α-Al_2O_3 from γ-Al_2O_3 were observed to result in Fe^{3+} ions incorporation in the lattice structure of γ-Al_2O_3, and then formation of the Fe-rich clusters within the γ-Al_2O_3 matrix, which increased the phase transformation rate to α-Al_2O_3 [15]. The enhanced formation mechanism of α-Al_2O_3 by doping with Fe^{3+} in this study agrees with the above findings. The hematite phase was not detected by XRD and no exothermic peak due to hematite crystallization (at 400–800 °C) was observed. It was found [16] that α-Al_2O_3 phase transformation was dominated by Al^{3+} diffusion. For boehmite co-doped with 1 mol% Ti^{4+} and 5 mol% Fe^{3+} (sample 1T), the phase transformation temperature further decreased to 1030 °C (Fig. 1(d)). This agrees with literature [17] that Ti^{4+} entered Al_2O_3 substitutionally, which resulting in the increase in V_{Al}''' concentration, thereby promoting $\gamma \rightarrow \alpha$-$Al_2O_3$ phase transformation. The broad exothermic peak observed at 700–900 °C can be ascribed to $\gamma \rightarrow \delta \rightarrow \theta$-$Al_2O_3$ phase transformation, which can be confirmed by XRD results shown in Fig. 2. For sample 1T added with K_2SO_4, 1T4K, the endothermic peak occurring at about 598 °C is associated with the transformation from the

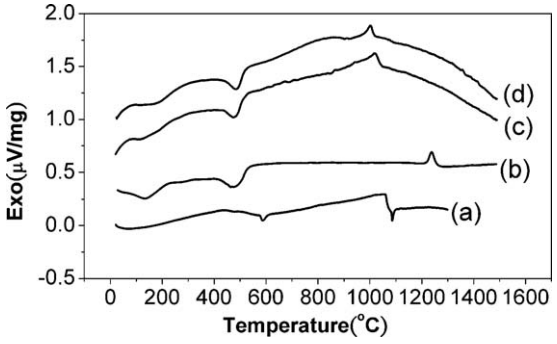

Fig. 1. DTA curves for boehmite added with various Fe^{3+}, Ti^{4+}, and K_2SO_4 molar ratios (a) 1T4K, (b) boehmite, (c) 0T and (d) 1T.

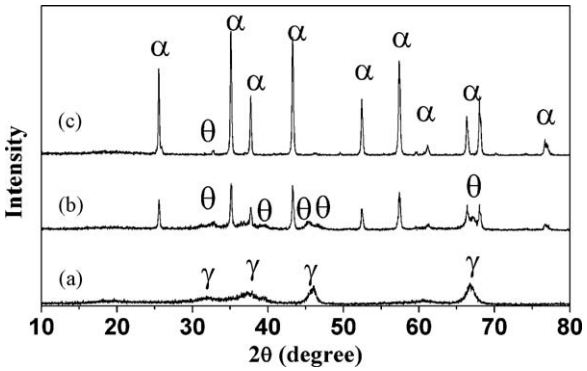

Fig. 2. XRD patterns for sample 1T calcined at various temperatures (a) 800 °C, (b) 900 °C and (C) 1000 °C (α,α-Al_2O_3, θ,θ-Al_2O_3, γ,γ-Al_2O_3).

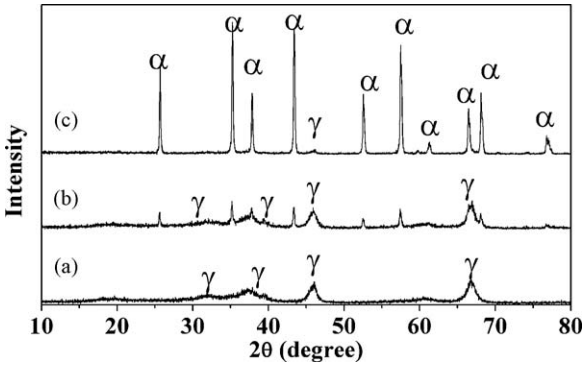

Fig. 3. XRD patterns for sample 0T4K calcined at various temperatures (a) 800 °C, (b) 900 °C and (C) 1000 °C (α,α-Al_2O_3, θ,θ-Al_2O_3, γ,γ-Al_2O_3).

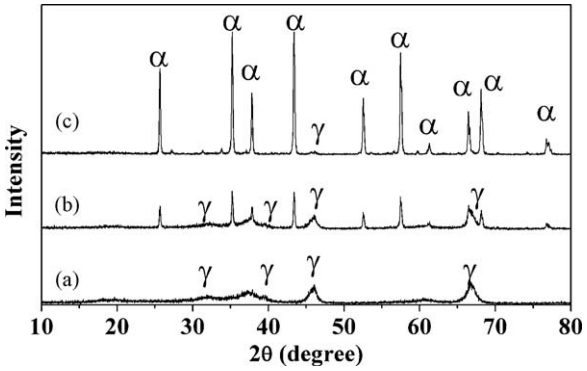

Fig. 4. XRD patterns for sample 1T4K calcined at various temperatures (a) 800 °C, (b) 900 °C and (C) 1000 °C (α,α-Al_2O_3, θ,θ-Al_2O_3, γ,γ-Al_2O_3).

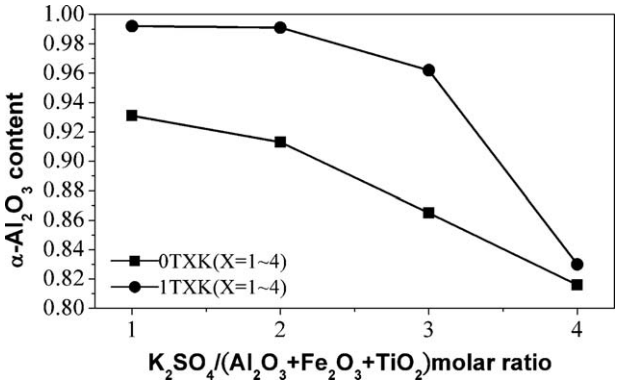

Fig. 5. Effect of different added molar ratio of potassium sulfate on α-Al_2O_3 formation.

orthorhombic (low temperature form) to the hexagonal phase (high temperature form) of K_2SO_4, the endothermic peak at 1067 °C is due to the melting of K_2SO_4, and no other exothermic peak originated from Al_2O_3 phase transformation was observed (Fig. 1(a)). Figs. 3 and 4 show the XRD patterns for samples 0T4K and 1T4K calcined at various temperatures. Comparison of the XRD patterns for the samples with and without K_2SO_4 addition (Figs. 2–4), shows that K_2SO_4 addition changed Al_2O_3 phase transformation from $\gamma \rightarrow \delta \rightarrow \theta \rightarrow \alpha$-$Al_2O_3$ to $\gamma \rightarrow \alpha$-$Al_2O_3$, avoiding the transition via θ-Al_2O_3.

3.2. Effects of addition of K_2SO_4 on the formation and anisotropy of α-Al_2O_3

Fig. 5 shows the effect of different added molar ratio of potassium sulfate on α-Al_2O_3 formation. The results indicate that the amount of α-Al_2O_3 formation decreased gradually with increasing K_2SO_4 addition of. It was found [18] θ- to α-phase transformation of Al_2O_3 to occur when θ-Al_2O_3 crystallite exceeds a critical size d_c, $\theta = 20$–25 nm upon heating to a temperature above 1000–1150 °C. Recently, many researches have added a salt as a diluent to the starting materials and then calcined the mixture at temperatures below the salt melting temperature [19–20]. It was found that salt can separate the nano-particles and prevent crystallite growth and agglomera-

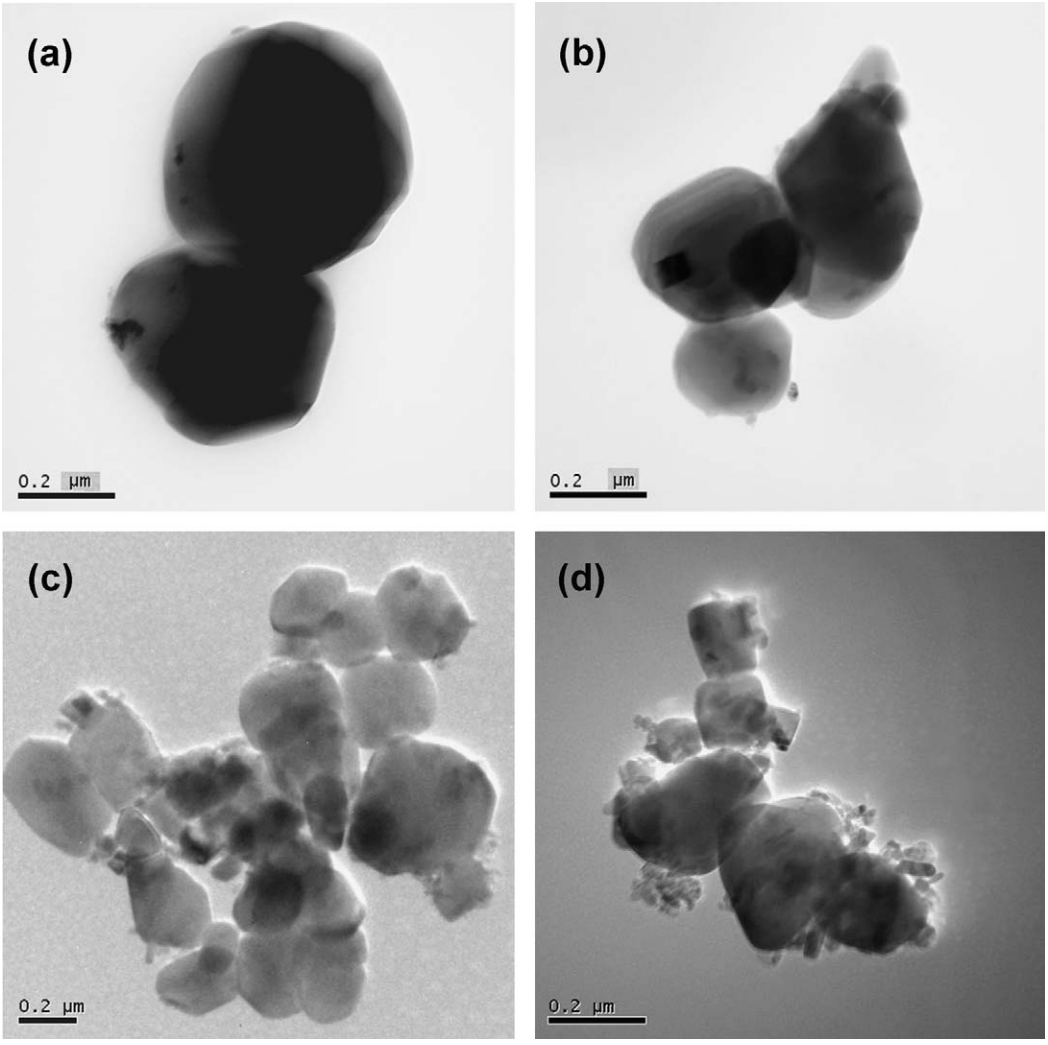

Fig. 6. TEM micrographs of sample 1T added with various K_2SO_4 molar ratios and calcined at 1000 °C for 2 h (a) 1T1K, (b) 1T2K, (c) 1T3K and (d) 1T4K.

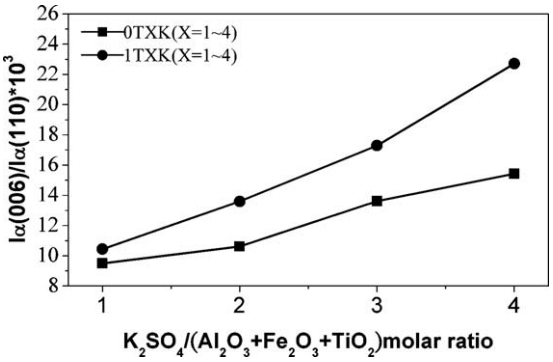

Fig. 7. Variation of $I_{(0\,0\,6)}/I_{(1\,1\,0)}$ for the samples with various amounts of K_2SO_4.

tion. The effect of monovalent cation additives on $\gamma \rightarrow \alpha$-$Al_2O_3$ was found to form a surface amorphous phase formed by the addition of K^+ cations which suppresses the growth of γ-Al_2O_3 grains and retards α-Al_2O_3 formation [21]. Because the calcination temperature (1000 °C) was below the K_2SO_4 melting temperature (1067 °C) in this study, K_2SO_4 may act as a solid barrier to separate γ-Al_2O_3 and to prevent crystallite growth, resulting in some γ-Al_2O_3 crystallites not reaching the critical phase transformation size, thereby surviving after calcination. Fig. 6 shows TEM micrographs of sample 1T added with various K_2SO_4 molar ratios and calcined at 1000 °C for 2 h. For sample 1T1K, the powders consist of crystallites 0.4–0.5 μm in size, which are opaque to electrons. With increasing potassium sulfate addition, the electron transparency of the crystallites increased, indicating the crystallite shape to gradually change from granular to flaky. In addition, for sample 1T4K, the proportion of the γ-Al_2O_3 crystallites with size less than 20 nm is higher than for the other samples, which is consistent with the XRD result (Fig. 4). The α-Al_2O_3 shape anisotropy can be semi-quantitatively determined by calculating $I_{(0\,0\,6)}/I_{(1\,1\,0)}$, where $I_{(0\,0\,6)}$ and $I_{(1\,1\,0)}$ are the integrated XRD intensities of the (0 0 6) peak and (1 1 0) peak of α-Al_2O_3, respectively. Fig. 7 shows the variation of $I_{(0\,0\,6)}/I_{(1\,1\,0)}$ for samples with various amounts of K_2SO_4, showing that the α-Al_2O_3 shape anisotropy increased with increasing K_2SO_4 addition. From the above results, it can be concluded that K_2SO_4 addition acts as a diluent to separate the nanoparticles

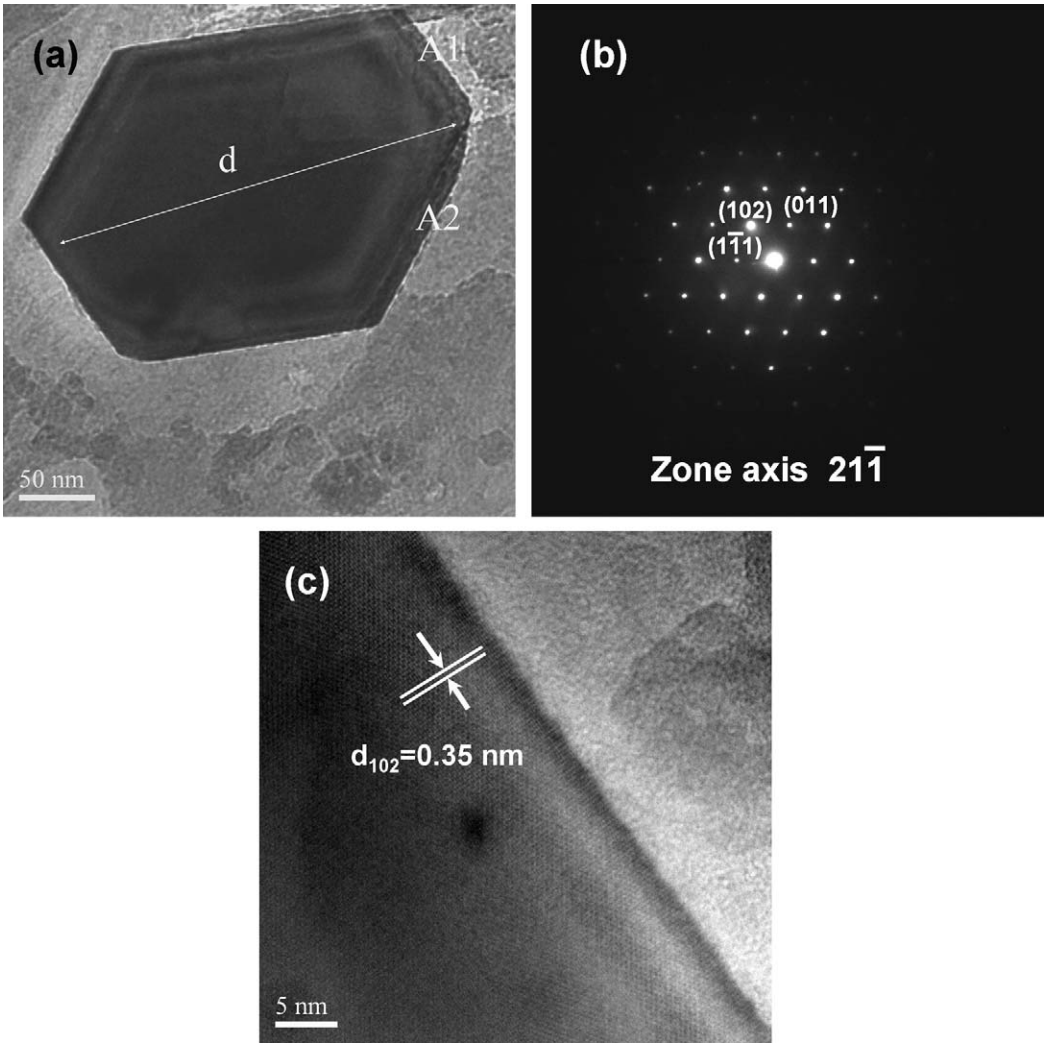

Fig. 8. (a) TEM bright field image, (b) corresponding to selected area of the electron diffraction pattern and (c) high resolution lattice image at A1 for sample 0T4K.

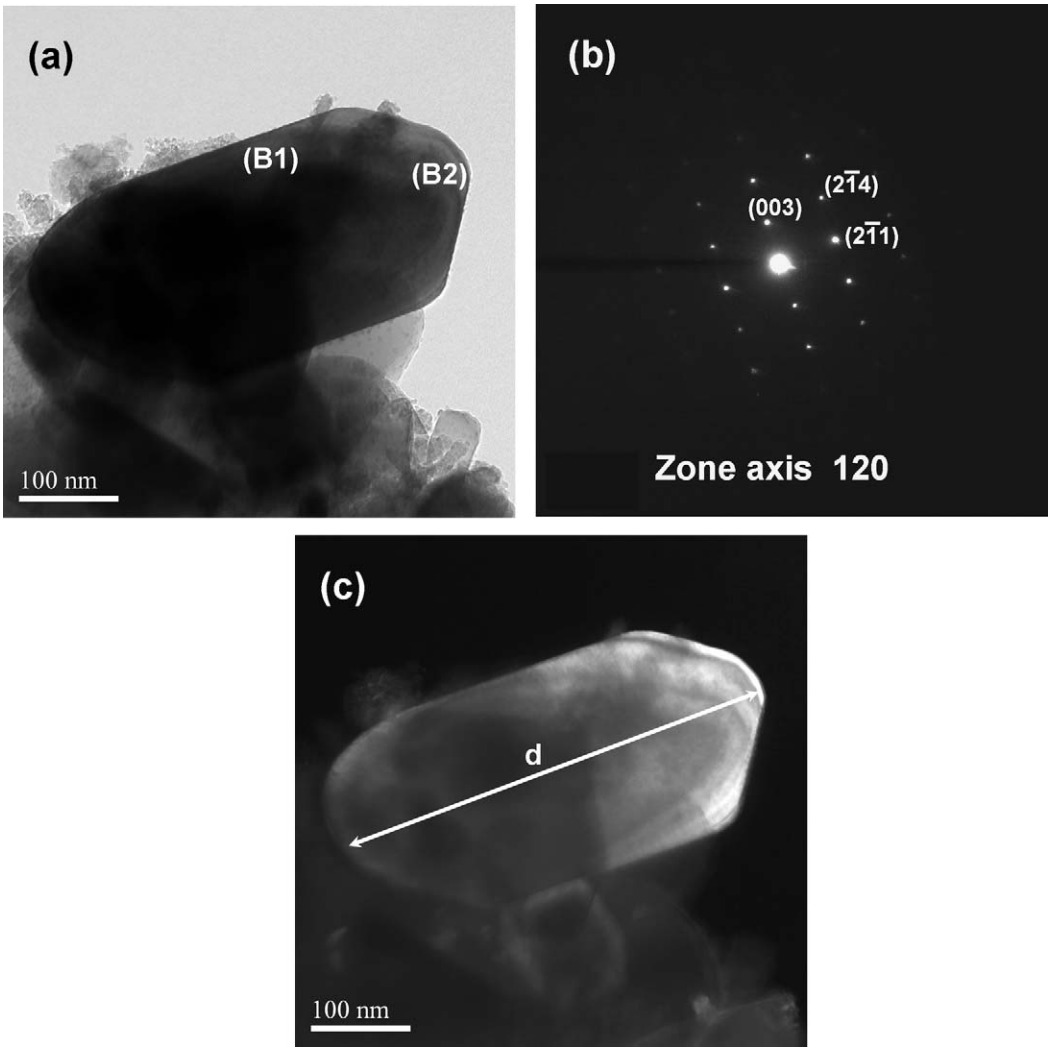

Fig. 9. (a) a TEM bright field image, (b) corresponding to selected area of the electron diffraction pattern (SAEDP) and (c) dark field image for sample 1T4K calcined at 1000 °C for 2 h.

and prevent crystallite growth and also promotes the anisotropic crystallite growth, thereby enhancing flaky α-Al_2O_3 crystallite formation.

3.3. Effect of Ti^{4+} addition on the anisotropic crystallite growth

Fig. 8(a and b) shows a TEM bright field image and corresponding selected area electron diffraction pattern (SAEDP) for sample 0T4K, respectively. The regular hexagonal pattern and strong diffraction spots indicate an excellent single crystal structure in the platelet, which could be indexed as α-Al_2O_3. Fig. 8(c) shows the high-resolution lattice image at A1 (in Fig. 8(a)) with a clearly resolved lattice fringe of the (1 0 2) planes (d = 0.348 nm), further confirming the single crystalline nature of each flaky crystallite. Moreover, the chemical composition of this region, as confirmed by EDS is shown in Table 2, which is close to the nominal composition. Fig. 9(a–c) shows a TEM bright field image, corresponding selected area electron diffraction pattern (SAEDP), and dark field image for sample 1T4K calcined at 1000 °C for 2 h, respectively, indicating the hexagonal flaky crystallite to be a single α-Al_2O_3 crystal. Comparison of Figs. 8 and 9 indicate that Ti^{4+} addition can promote the anisotropic crystallite growth of flaky α-Al_2O_3. Fig. 10 shows the high-resolution lattice image at B1 and B2 (in Fig. 9(a)) with a lattice fringe of the (0 0 3) planes (d = 0.43 nm) and (2–11) planes (d = 0.234 nm). In addition, the chemical composition of this region was confirmed by EDS and shown in Table 2. These results indicate that Ti^{4+} ions tend to segregate onto the surface of (0 0 3) basal planes, which promotes the anisotropic crystallite growth. This

Table 2
Chemical compositions of the different regions detected by EDS.

Area	Element (atom%)		
	Al K	Ti K	Fe K
Al	93.86	–	6.14
Bl	88.33	5.00	6.67
B2	91.65	1.31	7.04

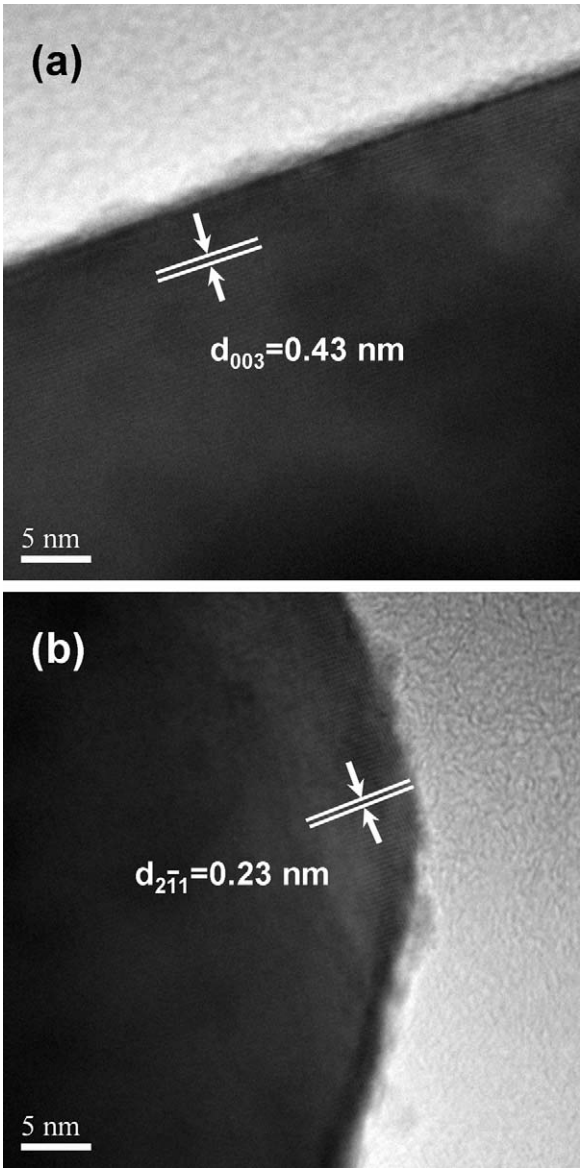

Fig. 10. High-resolution lattice image at (a) B1 and (b) B2 (in Fig. 9(a)) with a lattice fringe of the (0 0 3) planes (d = 0.43 nm) and (2 $\bar{1}$ 1) planes (d = 0.234 nm).

is supported by precious findings [22] indicating the tendency of TiO_2 to segregate at the grain boundary where it may hinder the growth of specific surfaces, thereby enhancing the development of platelet-shaped alumina grains.

4. Conclusions

i. Flaky single-crystal α-Al_2O_3 can be obtained by heating a mixture of Fe^{3+}-doped boehmite and potassium sulfate at 1000 °C.
ii. K_2SO_4 addition acts as a diluent to separate the nanoparticles and prevent crystallite growth, and also promotes the anisotropic crystallite growth.
iii. Ti^{4+} ions tend to segregate onto the surface of (0 0 3) basal planes, which promotes anisotropic crystallite growth, thereby enhancing flaky α-Al_2O_3 crystallite formation.

Acknowledgements

This work was financially co-sponsored by the Ministry of Economic Affairs of the Republic of China through contract (92-EC-17-A-08-S1-023) and National Science Council of the Republic of China (NSC94-2216-E-006-026).

References

[1] K.H. Heussner, N. Claussen, Yttria- and ceria-stabilized tetragonal zirconia polycrystals (Y-TZP, Ce-TZP) reinforced with Al_2O_3 platelets, J. Eur. Ceram. Ceram. Soc. 5 (1989) 193–200.
[2] H.C. Yuen, W.B. Lee, B. Ralph, Hot-roll bonding of aluminum–matrix composites with different volume fractions of alumina, J. Mater. Sci. 30 (4) (1995) 843–848.
[3] J. Block, J.W.K. Lau, Thermally conductive elastomer containing alumina platelets, US patent 5,137,959.
[4] N. Katuhisa, Flaky aluminum oxide and pearlescent pigment and production thereof, EP patent, 0763573A3.
[5] R.F. Hill, R. Danzer, R.T. Paine, Synthesis of aluminum oxide platelets, J. Am. Ceram. Soc. 84 (3) (2001) 514–520.
[6] C.A. Shaklee, G.L. Messing, Growth of α-Al_2O_3 platelets in the HF-γ-Al_2O_3 system, J. Am. Ceram. Soc. 77 (11) (1994) 2977–2984.
[7] X. Jin, L. Gao, Size control of α-Al_2O_3 platelets synthesized in molten Na_2SO_4 flux, J. Am. Ceram. Soc. 87 (4) (2004) 533–540.
[8] S. Hashimoto, A. Yamaguchi, Synthesis of α-Al_2O_3 platelets using sodium sulfate flux, J. Mater. Res. 14 (12) (1999) 4667–4672.
[9] S. Hashimoto, A. Yamaguchi, Formation of porous aggregations composed of Al_2O_3 platelets using potassium sulfate flux, J. Eur. Ceram. Soc. 19 (1999) 335–339.
[10] N.S. Bell, S.B. Cho, J.H. Adair, Size control of α-alumina particles synthesized in 1,4 butanediol solution by α-alumina and α-hematite seeding, J. Am. Ceram. Soc. 81 (6) (1998) 1411–1420.
[11] M. Wei, K.L. Choy, Novel synthesis of α-alumina hexagonal nanoplates using electrostatic spray assisted chemical vapor deposition, Nanotechnology 17 (2006) 181–184.
[12] H.C. Park, S.W. Kim, S.G. Lee, J.K. Kim, S.S. Hong, G.D. Lee, S.S. Park, Synthesis of α-alumina platelets using flux method in 2.45 GHz microwave field, Mater. Sci. Eng. A 363 (2003) 330–334.
[13] H.I. Hsiang, T.H. Chen, C.C. Chuang, Synthesis of α-Al_2O_3 hexagonal platelets using a mixture of boehmite and potassium sulfate, J. Am. Ceram. Soc. 90 (12) (2007) 4070–4072.
[14] J.L. McArdle, G.L. Messing, Transformation, Microstructure development, and densification in α-Fe_2O_3-seeded boehmite-derived alumina, J. Am. Ceram. Soc. 76 (1) (1993) 214–222.
[15] G.C. Bye, G.T. Simpkin, Influence of Cr and Fe formation of α-Al_2O_3 from γ-Al_2O_3, J. Am. Ceram. Soc. 57 (8) (1974) 367–371.
[16] K. Okada, A. Hattori, Effect of divalent cation additives on the γ-Al_2O_3 to α-Al_2O_3 phase transition, J. Am. Ceram. Soc. 83 (4) (2000) 928–932.
[17] A.G. Alejandre, M.G. Cruz, M. Trombetta, Characterization of alumina-titania mixed oxide supports Part II: Al_2O_3-based supports, Microporous Mesoporous Mater. 23 (1998) 265–275.
[18] H.L. Wen, F.S. Yen, Growth characteristics of boehmite-derived ultrafine theta and alpha-alumina particles during phase transformation, J. Cryst. Growth 208 (2000) 696–708.
[19] J. Ding, T. Tsuzuki, P.G. McCormick, Ultrafine alumina particles prepared by mechanochemical/thermal processing, J. Am. Ceram. Soc. 79 (11) (1996) 2956–2958.
[20] Y.X. Li, W.F. Chen, X.Z. Zhou, Z.Y. Gu, C.M. Chen, Synthesis of CeO_2 nanoparticles by mechanochemical processing and the inhibiting action of NaCl on particle agglomeration, Mater. Lett. 59 (2005) 48–52.
[21] K. Okada, A. Hattori, Y. Kameshima, A. Yasumori, R.N. Das, Effect of monovalent cation additives on the γ-Al_2O_3 to α-Al_2O_3 phase transition, J. Am. Ceram. Soc. 83 (5) (2000) 1233–1236.
[22] D.S. Horn, G.L. Messing, Anisotropic grain growth in TiO_2-doped alumina, Mater. Sci. Eng. A 195 (1995) 169–178.